Hydrophobic eutectogels: a new outfit for non-ionic eutectic solvents

G. de Araujo Lima e Souza [a], M.E. Di Pietro [a, *], V. Vanoli [a], W. Panzeri [b], F. Briatico-Vangosa [a], F. Castiglione [a], A. Mele [a, b]

[a] Department of Chemistry, Materials and Chemical Engineering "G. Natta', Politecnico di Milano, Piazza Leonardo da Vinci 32, 20133, Milano, Italy
[b] CNR-SCITEC Istituto di Scienze e Tecnologie Chimiche, Via A. Corti 12, 20133, Milano, Italy

A B S T R A C T

Hydrophobic non-ionic eutectogels (HEG) are prepared for the first time from hydrophobic non-ionic (type V) eutectic solvents (HES) in a simple one-pot procedure with a low-cost low molecular weight gelator. Stable and homogeneous gels were obtained in a matter of minutes at a very low loading, with a preparation process ranked as "excellent" in the EcoScale metrics. We illustrate that the liquid-like nature of the hydrophobic mixture is retained upon gelation. From a physicochemical viewpoint, the major finding is the unexpected increase of the diffusive motion of the components in the HEG compared to pure HES. In one case, two populations corresponding to fast and slow diffusion components have been detected. These features of HEG overall open up new horizons toward technological applications requiring solid-like, yet mobile systems, and could promote their usage on a large scale.

1. Introduction

Deep eutectic solvents (DES) are eutectic mixtures of (at least) two components showing significant negative deviations from thermodynamic ideality, mainly ascribable to a hydrogen bond network between the components [1]. DES are classified into five different types (I–V) according to the nature of their hydrogen bond donors (HBDs) and acceptors (HBAs) (Table S1) [2]. Recently, the fascinating subclass of type V hydrophobic DESs [3], composed only of neutral compounds with a high degree of hydrophobicity, have stepped into the spotlight of materials science [1,2,4,5]. Given the misconception of the (D)ES definition, we use here the catch-all term hydrophobic eutectic solvents (HES, see the SI for a disambiguation on terminology) [6]. HES share the convenient synthesis and low ecological footprint of DES, being easily prepared with 100% atom economy from readily available, low-cost and mainly non-toxic and biodegradable precursors such as terpenes and fatty acids [2]. The lower viscosity of HES compared to conventional DES is an added value [2,7]. Structurally, this stems from the presence of weaker interactions compared to ionic DES, that lead to slight – or even negligible – deviations from the eutectic temperature of an ideal mixture [8]. All in all, this makes HES an economically and environmentally sustainable choice for many technological applications [1,5,9–11]. Yet, various specific fields, from biomedical to electrochemistry, require the immobilization of the solvent in a solid-like scaffold, while keeping its properties of liquid phase [12,13]. To this purpose, a suitable strategy is the formation of gels, where a three-dimensional solid-like network permeates throughout the liquid-like medium [14]. Widely employed for ionic liquids [15,16], this approach has been recently applied also to DESs – mainly type III and IV – forming so-called eutectogels [17–21]. Structured, gel-like systems have been prepared immobilizing DESs in silica matrices, biopolymers, or other cross-linked/entangled polymers [18,21]. Colloidal gels have also been reported after dispersion of nanoparticles in DES [18]. Conceptually different strategies consist in polymerizing deep eutectic monomers [22,23], or using DES itself as a supramolecular gelator [24,25], but both methods alter considerably – chemically or physically – the DES structure, hence the intrinsic properties of the liquid phase are not preserved.

A particularly promising approach to confine a eutectic solvent in a supramolecular gel is based on the ability of low-molecular-weight gelators (LMWGs) to form self-assembled nanostructures underpinned solely by reversible noncovalent interactions [26–36]. Most notable among them is 1,3:2,4-dibenzylidene-*D*-sorbitol (DBS), a

low-cost, commercially available building block, whose versatility makes it the closest example to a universal gelator [37,38]. DBS has been reported to self-assemble into nanofibrils through self-complementary H-bond and π stacking in hydrophilic type III DES composed of an organic salt (choline chloride, ChCl) and alcohols/urea as the HBD [39]. Unfortunately, loadings of at least 3% w/v were required in all systems to promote the DBS self-assembly [39]. As chloride anion is known to establish H-bonds with hydroxyl groups [40], the presence of the ionic species ChCl likely suppresses the gel formation due to interaction of chloride anion with the hydroxy groups on DBS [39]. Halogenated DBS (X-DBS) have been recently synthetized to improve the gelation ability in ChCl-DES [41].

In this Communication, we introduce the hydrophobic eutectogels HEG as a novel class of fully non-ionic supramolecular gels based on HES. The choice is motivated by (i) the non-hygroscopic nature and water-immiscibility of HES, beneficial features for actual technological applications [2,18], and (ii) the absence of ionic species, which may either interfere strongly with the gelator (e.g. chloride) or be potentially toxic and hazardous (e.g. metal salts) [18,39]. We selected seven systems as a paradigmatic set (Table 1 and S4), including the prototypical hydrophobic DES menthol:thymol [3,8], and various already reported hydrophobic eutectic mixtures obtained combining menthol, thymol and long alkyl chain carboxylic acids [42,43]. Albeit the formation of a gel stable up to 41 °C has been reported in menthol:lauric acid 1:1 after addition of 0.9 w/v% of the ionic liquid crystal 1-hexadecyl-3-methylimidazolium bromide [44], to the best of our knowledge there is no systematic report of supramolecular gels formed in hydrophobic non-ionic eutectic systems by self-assembly of a non-ionic LMWGs to date. The model set of HEG is evaluated at the macroscopic and microscopic level, confirming that all systems are gels and showing that the liquid-like nature is retained within the gel scaffold. As a major finding, we show that the diffusivity of the components is surprisingly enhanced with respect to the pristine HES, which is totally counterintuitive and highly advantageous for future applications. The correlation between diffusivity enhancement and strength of interactions is discussed. A peculiar diffusive behavior emerges for one system, where two populations – corresponding to fast and slow diffusion components – are detected after gelation.

2. Materials and methods

The systems selected for the present study are listed in Table 1.

The simple one-step HEG preparation consists in dissolving the proper amounts of DBS in the HES under stirring at a specific temperature until the mixture turns transparent, indicating the entire solubilization of the gelator. Experimental details on the preparation protocol, including a summary of all the HES and HEG here discussed, are given in the ESI.

3. Results and discussion

The gelation of the non-ionic HEG takes less than 10 min, hence more than six times faster than ChCl-based eutectogels under the same conditions [39]. The absence of chloride anion in the matrix favours the self-assembling [39], making HES excellent media for supramolecular eutectogels. For most HES, gelation successfully occurred with only 1% w/w of DBS – exceptions being Men:Thy and Thy:CapA – hence even better than most gels of X-DBS in ChCl-DES [41]. For all systems, stable homogeneous gels were formed at 2%, 5% and 8% of DBS loading (Fig. S2), as assessed by the tube inversion method [33]. A systematic study of DBS gelation in HES is crucial, as species are held together by noncovalent interactions that may interfere with self-assembly of the gelator into a nanoscale network [39], and such behavior is not easily predictable in unconventional solvents (see SI) [37].

Table 1
Selected systems used for the preparation of the hydrophobic eutectogels.

Eutectic mixture	Molar ratio	Abbreviation
menthol:thymol	1:1	Men:Thy
menthol:stearic acid	1:1	Men:SteA
menthol:lauric acid	2:1	Men:LauA
menthol:caprylic acid	1:1	Men:CapA
lauric acid:caprylic acid	1:3	LauA:CapA
thymol:lauric acid	0.55:0.45	Thy:LauA
thymol:caprylic acid	1:1	Thy:CapA

The sol-gel transition temperatures (T_{gel}, Fig. 1a) of all HEG, measured via the tube inversion method [33], are in line or higher than DBS-eutectogels in ChCl-based DES [39,41]. As expected, the T_{gel} value increased with DBS content, indicating that a more effective self-assembling network is established with increasing gelator concentration [39]. For the systems containing 8% of DBS, the T_{gel} followed the order Men:SteA (153 °C) > LauA:CapA (142 °C) > Men:LauA = Men:CapA (140 °C) > Men:Thy (125 °C) > Thy:LauA (119 °C) > Thy:CapA (110 °C). The lower hydrogen bond donor ability of Men-based HES – as expressed by the value of Kamlet-Taft parameter α (0.68–0.85) [42] – can explain their more efficient gelation ability when compared to the Thy-based HES (α in the range 1.05–1.10) [42] (see the SI for a discussion on the correlation between gelation ability of DBS and Kamlet-Taft parameters of HES) [37].

The series of HEG with the highest T_{gel}, that is containing 8% of DBS (Fig. 2), was the model set for physico-chemical characterization. For clarity, the gelator content (% w/w) is indicated after the composition (e.g. Men:CapA-DBS8).

To investigate the mechanical properties, rheological measurement were performed on the seven HEG molded into disk-shaped samples. All HEG were confirmed to be gels with the storage modulus G′ larger than the loss modulus G″ (a representative frequency sweep experiment is displayed in Fig. 3a). The measured G′ values were not dependent on the angular frequency, thus further confirming the formation of a gel. Gels with comparable G′ and G″ values were obtained after heating-cooling cycle, confirming their thermoreversibility (Fig. S4). The G′ values at 60 °C ranged from 1.8×10^6 Pa in LauA:CapA-DBS8 to 1.7×10^7 Pa in Men:SteA-DBS8 (Fig. S5), indicating overall stiff gels. Gels broke down with increasing shear strain amplitude, as shown by the G′-G″ crossover, but they could reform when shear strain amplitude was reduced, showing self-healing properties (Fig. 3b).

Thermogravimetric analysis (TGA) was performed on HEG-DBS8 and the corresponding pristine HES. TGA and DTG thermograms are displayed for all samples in Fig. 1b and Figs. S6–S13, and the corresponding degradation temperatures are listed in Table S5. All HEG, but Men:SteA-DBS8, presented a similar degradation profile with a two-step weight loss (Fig. 1b), the first corresponding to the degradation of the HES, and the second representing the thermal degradation of the DBS. As expected, no weight loss due to water evaporation is observed. Thy:LauA and Thy:CapA show the highest operational temperature limit (T_d = 257 °C and 226 °C, respectively, Table S5), in agreement with previous findings [45]. Comparing the thermograms of each pair HES/HEG, it emerges that the formation of a supramolecular gel lowers the thermal stability of Thy:LauA and Thy:CapA (reduction of 25–30 °C), whereas substantially it does not affect the degradation temperature of the other systems. Men:SteA stands out, as an additional plateau is observed in the thermograms of both HES and HEG (Fig. S8). The first two plateaux may be interpreted as separate degradations of the two HES components [8], due to the weak Men-SteA interactions [42], flanked by the rather intense SteA-SteA dispersive interactions. Application-

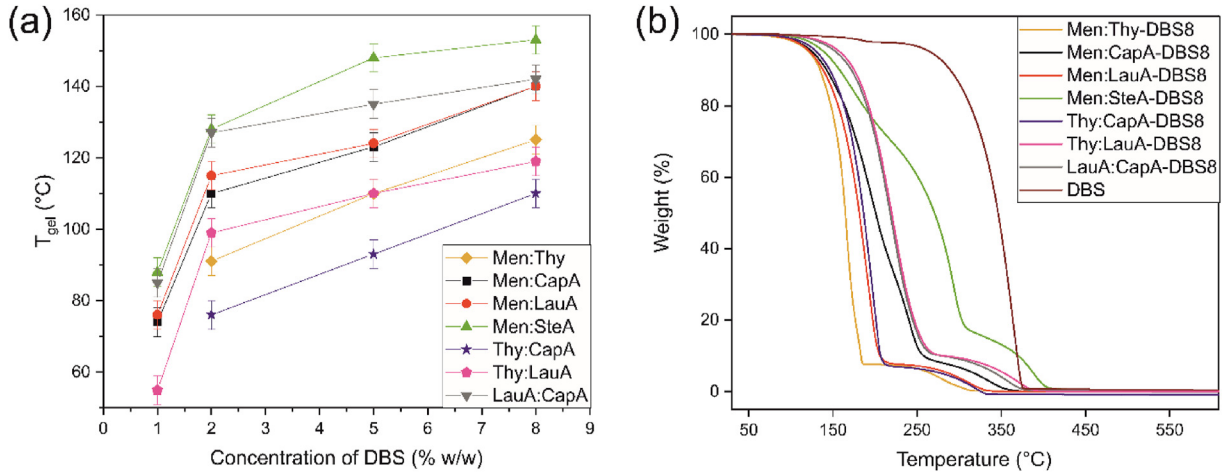

Fig. 1. (a) T_{gel} values (with lines as guide to the eye) of the studied HEG determined via reproducible tube inversion experiments. (b) TGA thermograms of the model set of HEG-DBS8. The thermogram of DBS is also reported as reference.

wise, all systems are stable up to 150 °C, in line with (or even higher than) state-of-the-art DES-based gels [46,47], establishing then relatively high boundary limits for a large usage.

The promising macroscopic properties of the novel HEG motivated a study of the molecular organization and intermolecular interactions. A first insight was achieved via ATR-FTIR of the selected HEG and comparison with both the corresponding HES and the pure components (Figs. S14–S20). Two main spectral regions – the hydroxyl stretching region (3000–3700 cm^{-1}) and carbonyl stretching region (1600–1800 cm^{-1}) – were found to be particularly subjected to variations (Fig. 4). In all Men- and Thy-based HES, the band corresponding to O–H stretching (observed at 3304 cm^{-1} and 3169 cm^{-1} in the pure components, respectively) broadens and shifts to higher wavenumbers. Additionally, a minor hypsochromic shift is observed for the C=O stretching peak of fatty acids in most HES, except for Thy:CapA and LauA:CapA. Overall, these observations indicate the occurrence of hydrogen bonds in the vicinity of these functional groups [24,25]. Noteworthy, the ATR-FTIR spectra of HEG are very close to those of the corresponding HES, indicating that the overall intermolecular network is not remarkably affected by the gelator. As expected, the spectral regions at 900-1200 cm^{-1} and 600-900 cm^{-1}, attributed to the C–O–C and aromatic groups of DBS [48], are preserved in the FTIR spectra of the eutectogels (Figs. S14–S20).

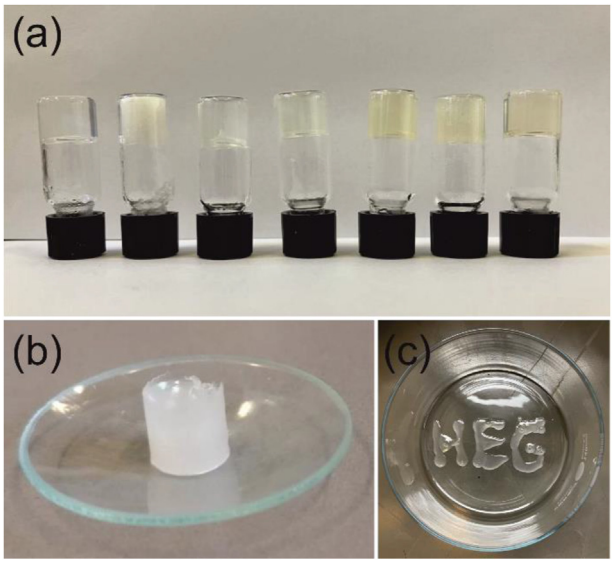

Fig. 2. (a) Set of HEG with 8% DBS (HEG-DBS8); (b) photograph of Men:Thy-DBS8; (c) photograph of Men:CapA-DBS8.

Liquid state and high-resolution magic angle spinning (HRMAS) NMR spectroscopy were then applied to the neat HES and the corresponding HEG, respectively. The NMR studies in the pure components are a fingerprint of the structural and dynamic features of the HES/HEG with no interference from solvent and/or dilution effects. No relevant changes of the spectral profile of the HES were detected in the 1D ^{1}H NMR spectra after gelation (Figs. S21–S27), in agreement with previous results on ChCl-based DBS self-assembled gels [39]. This supports the view of HEG as a physical gel retaining the liquid-like nature of its parent HES. A closer inspection reveals, however, that some samples showed the exchangeable proton signal slightly shifted upfield (i.e., at lower chemical shifts) on passing from the HES to the corresponding HEG (Fig. 5a, Fig. S28). According to the magnitude of such *gelation-induced chemical shift variation* Δδ, Thy:CapA, Thy:LauA and LauA:CapA would be ranked as "responsive" to DBS interference ($\Delta\delta > 0.35$), while Men:LauA, Men:SteA and Men:Thy as "robust" ($\Delta\delta < 0.1$). It is known that the upfield shift of ^{1}H resonances is symptomatic of the weakening of the H-bond to electronegative atoms, which translates into an increase in the shielding of corresponding proton [49]. Indeed, the chemical shift variation of the exchangeable proton signal in a given ES is a very strong indicator of weakening of the H-bonds in the network and their replacement with relatively less strong interactions [50,51]. Similarly, Δδ measured here can be correlated with the strength of the H-bond in the system, indicating that "responsive" HES, i.e. those more susceptible to perturbation, have a less stable network of intermolecular interactions than the "robust" HES. This partially overlaps the TGA results, with the T_d of Thy:CapA, Thy:LauA most affected by the presence of the gelator.

Given the importance of having favourable transport properties in view of potential applications of HEG, the apparent self-diffusion coefficients (D_i) of the different species (individual HES components and exchangeable proton) were measured via PFG-NMR (Table S6). Note that the self-diffusivity of the fast more abundant component is displayed for Men:SteA-DBS8 (vide infra). For a prompt comparison among the HES and HEG systems, averaged diffusivities D^{avg} were calculated by weighting on the mole fractions of the components (see SI) and are displayed in Fig. 5b. Remarkably, the diffusivity observed for HEG is in the typical range

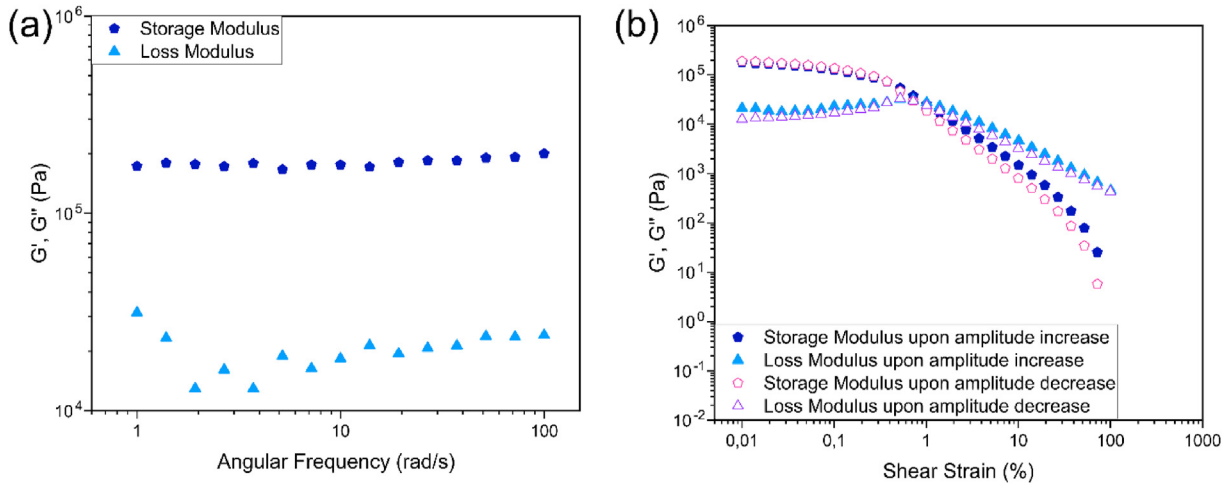

Fig. 3. (a) Angular frequency dependence of the storage modulus (G′, blue pentagons) and loss modulus (G″, light blue triangles) for LauA:CapA-DBS8 measured at 60 °C with a shear strain of 0.01%; (b) strain amplitude dependence of the storage modulus (G′, pentagon) and loss modulus (G″, triangle) measured for LauA:CapA-DBS8 at 60 °C with an angular frequency of 10 rad/s, upon increase from 0.01% to 100% (blue and light blues filled symbols) and decrease from 100% to 0.01% (pink and purple empty symbols) of the shear strain.

of liquid systems (2×10^{-10} - 2×10^{-11} m^2 s^{-1}), despite the quasi-solid appearance of the samples. Overall, Thy-based HES and HEG display higher D_i than the corresponding Men-based ones, due to the weaker hydrogen bonding network in the former ($D^{avg}_{Thy:CapA} > D^{avg}_{Men:CapA}$ and $D^{avg}_{Thy:LauA} > D^{avg}_{Men:LauA}$ for both HES, empty symbols, and HEG, filled symbols). A similar trend can be seen when considering the three systems containing the same fatty acid (LauA or CapA): in both the HES and the HEG systems $D^{avg}_{LauA:CapA} > D^{avg}_{Thy:LauA(CapA)} > D^{avg}_{Men:LauA(CapA)}$, indicating an overall strength of intermolecular forces following the reverse order Men:LauA(CapA) > Thy:LauA(CapA) > LauA:CapA.

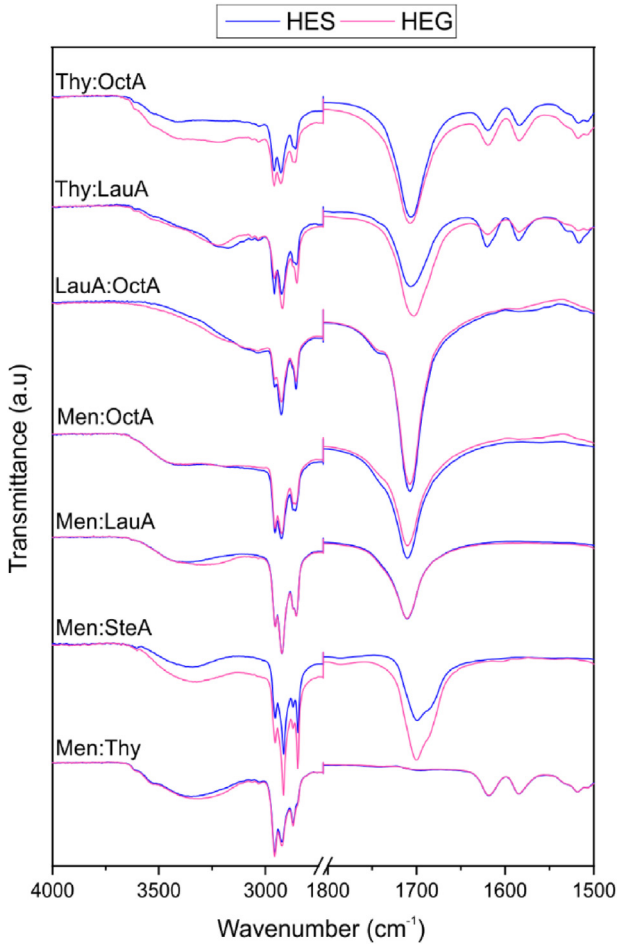

Fig. 4. ATR-FTIR spectra of all HES and HEG-DBS8. None of the signals were scaled but plotted as obtained after subtraction of the baseline.

Somehow counterintuitively, diffusivities of both components are higher in the HEG than in the HES (Table S6), except for Men:SteA where almost equal values were obtained. Apparently, the presence of a self-assembled gel-like network does not inhibit but indeed enhances translational motion of the molecules into the system, with an increase ranging from ca. 40% in Men:LauA (from $D^{avg}_{HES} = 3.9\times10^{-11}$ m^2 s^{-1} to $D^{avg}_{HEG} = 5.5\times10^{-11}$ m^2 s^{-1}) to almost 90% in Men:CapA (from $D^{avg}_{HES} = 7.2\times10^{-11}$ m^2 s^{-1} to $D^{avg}_{HEG} = 1.4\times10^{-10}$ m^2 s^{-1}). An increase in the apparent diffusion has been observed also after confinement of the hydrophilic DES ChCl:glycerol 1:2 in bacterial cellulose [52]. In that case, authors proposed an explanation based on a partial migration of chloride anions from the bulk to the polymer surface, with consequent reduction of interactions with choline and glycerol and displacement of residual water. In our case – HEG composed of non-ionic, chloride-free hydrophobic species – it can be hypothesized that, even if the HES components are only weakly interacting with DBS (see previous TGA and ATR-FTIR measurements), the sample-spanning network established by the supramolecular gelator reasonably acts as a perturbation on the local inter-HES interactions, resulting in an overall increased mobility of the HES species in system. A rearrangement of supramolecular networks has also been described in eutectogels of hydrophilic type III DES and xanthan gum [53]. Notably, both in Zeng et al. [53] and here, the effect of the gelator (xanthan gum and DBS, respectively) is inversely proportional to the strength of the interactions: HES having more unstable supramolecular network are more susceptible to interference from the self-assembling compound. Indeed, comparing Men- and Thy-based HES (i.e. Men:LauA vs Thy:LauA and Men:CapA vs Thy:CapA), it emerges that the enhancement in the translational motion induced by gelation (i.e., the gap between empty and filled symbols for a given system, indicated as an arrow in Fig. 5b) correlates with the strength of the H-bond network: due

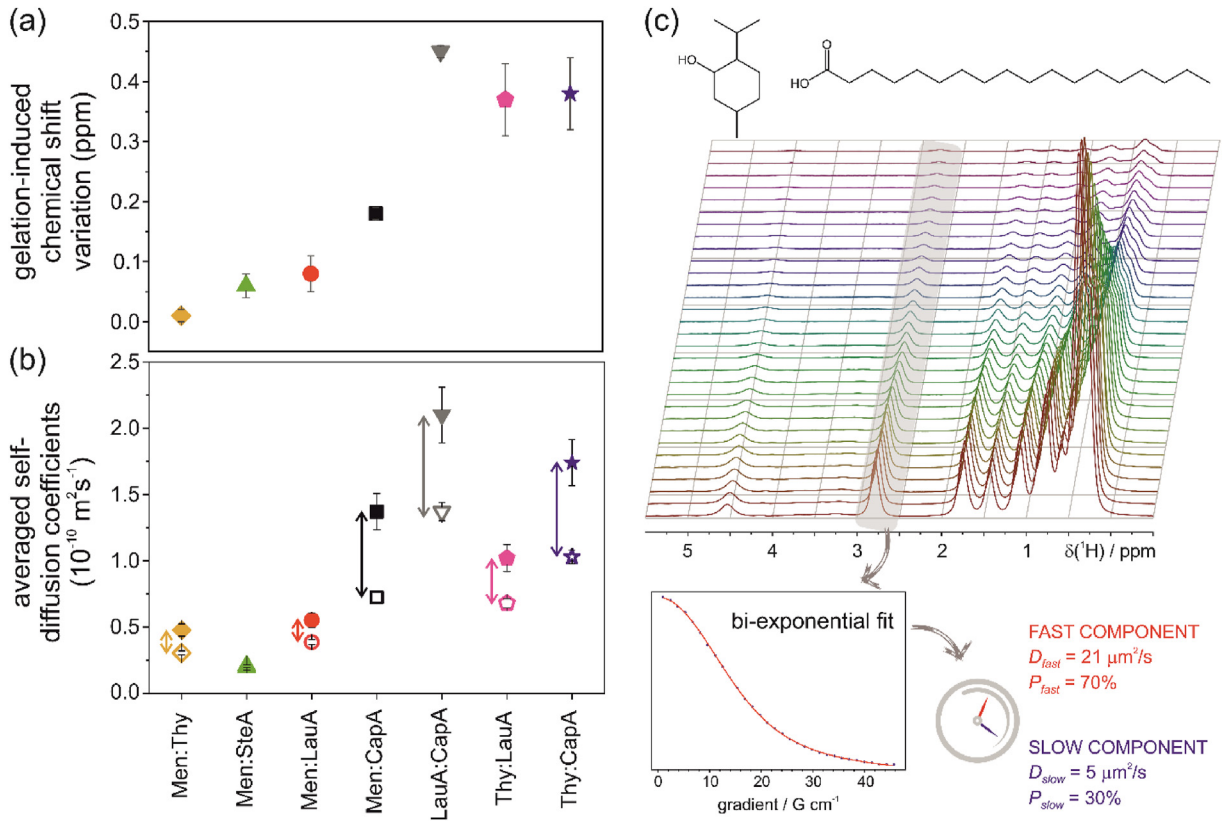

Fig. 5. (a) Gelation-induced chemical shift variation of the exchangeable proton signal (absolute value) observed between the 1D ^{1}H liquid-state NMR spectrum of HES and HRMAS NMR spectrum of the corresponding HEG. The quantity is defined as $\Delta\delta = |\delta(\mathrm{OH})_{\mathrm{HES}} - \delta(\mathrm{OH})_{\mathrm{HEG}}|$, and it is reported in ppm. (b) Averaged self-diffusion coefficients of the HES (empty symbols) and HEG (filled symbols) studied. The arrows are a graphic indication of the diffusivity enhancement observed on passing from the HES to the corresponding HEG. The self-diffusivity of the fast more abundant component is displayed for Men:SteA-DBS8. (c) Sketch of the flow-chart for extracting the fast and slow components of diffusivity in the case of Men:SteA-DBS8. The decay profiles from PFG-NMR experiments (298 K, 4 kHz spin rate) are fitted with a bi-exponential decay model thus affording D_{fast} and D_{slow} and the corresponding populations (P_{fast} and P_{slow}).

to the highest hydrogen bond donor ability of Thy, the difference in the averaged diffusivities of HEG and HES is higher for Thy-based HES ($D^{avg}_{\mathrm{HEG}} - D^{avg}_{\mathrm{HES}}$ equal to 3.5×10^{-11} m^2 s^{-1} for Thy:LauA and 1.7×10^{-11} m^2 s^{-1} for Men:LauA; $D^{avg}_{\mathrm{HEG}} - D^{avg}_{\mathrm{HES}}$ is 7.2×10^{-11} m^2 s^{-1} for Thy:CapA and 6.4×10^{-11} m^2 s^{-1} for Men:CapA). Notably, interactions other than H-bonds seem to play a role in explaining the diffusivity enhancement upon gelation. This effect is clearer if the experimental points of Fig. 5b are grouped in subsets. Looking at the Men-fatty acids systems (green triangles, red circles and black squares in Fig. 5b), it is observed that the enhancement in translational motion induced by gelation decreases with the increase of the alkyl chains, as it can be quantified using the ratio of the averaged diffusivities in HEG and HES systems: $D^{avg}_{\mathrm{HEG}}/\ D^{avg}_{\mathrm{HES}}$ is in the order Men:CapA = 1.9 > Men:LauA = 1.4 > Men:SteA = 1.0. The trend may be ascribed to the dispersive interactions, which get more pronounced with the increasing alkyl chain length from C8 to C18 [42]. The same holds true for Thy:CapA and Thy:LauA ($D^{avg}_{\mathrm{HEG}}/\ D^{avg}_{\mathrm{HES}}$ equal to 1.7 and 1.5, respectively). Overall, this picture matches that derived from the gelation-induced shift of the exchangeable protons in Fig. 5a, supporting the idea of an interference of DBS gelation upon HES-HES interactions inversely proportional to either the strength of the pre-existing H-bond interactions or the number of C atoms of the alkyl chains, in turn related to the strength of the dispersive forces. Drawing definite conclusions on the effect of the DBS on the mobility of the species needs further investigations and it is not trivial to disentangle the contribution coming from intermolecular network (including both H-bonds and dispersive forces) from the inherent size-dependent motion. The main indication here is a non-random enhancement of the diffusion after gelation, which would be beneficial in applications where promotion of transport is desirable.

Finally, Men:SteA-DBS8 deserves special mention. In general, when running PFG-NMR experiments to extract the apparent diffusion coefficient, the signal intensity decays are fitted by a mono-exponential function, obtaining a single self-diffusion coefficient. In the case of Men:SteA-DBS8, the intensity decays of all signals surprisingly showed a bi-exponential profile (Fig. 5c and Fig. S31). Such a behavior is consistent with the co-presence of two diffusivity components (D_{fast} and D_{slow}), in turn related to two different populations experiencing different physical and chemical environments in the gel sample. The relative populations of roughly 70% and 30% for the fast and slow components, respectively, were obtained for Men:SteA-DBS8, with a small standard deviation (Table S8). The two populations do not correspond to the individual components Men and SteA (note for instance that even the signal at 3.0 ppm corresponding to H1 of menthol showed a bi-exponential decay, Fig. S31), but are rather the result of confinement/heterogeneity effects. Moreover, a mono-exponential model satisfactorily reproduced all signals of HES Men:SteA, indicating that a single pool of molecules exists in the eutectic mixture. Further investigations are currently in progress to unveil the molecular picture responsible for such diffusive behavior, and whether this is related to some extent to the three-step degradation profile of Men:SteA-DBS8.

After discussing the characterization of the HEG, we briefly address the sustainability based on the EcoScale metrics [54,55]. The detailed calculation of the ranking associated to each HEG

preparation is reported in Table S9. Briefly, and with reference to the original Van Akel paper, the categories Yield, Price, Technical setup, Workup and Purification did not introduce penalties. This is simply related to the absence of by-products, solvent and, consequently, solvent removal steps. Penalty points were only introduced for Thy-based systems due to its moderate toxicity and aquatic hazard. The energy consumption (heating < 1 h for the whole HEG set) introduced 2 penalty points for each HEG. Overall, the EcoScale ranking spanned the 93–98 points, thus placing the preparation process of the HEGs here considered at the "excellent" grade.

4. Conclusions

Hydrophobic non-ionic eutectogels are introduced as a new class of environmentally friendly and cost-effective materials obtained from the facile and effective immobilization of type V (deep) eutectic solvents by the gelator DBS. Prepared through a highly sustainable procedure (ranked as "excellent" in the EcoScale green metrics), the novel HEG reshape the unique economic and environmental benefits of the eutectic systems into quasi-solid gel-like materials, which do not suffer from water sorption and water miscibility issues. This makes them of potential interest for medical and biotechnological applications, as well as separation, extraction and purification processes. Due to weak interactions with the scaffold, the liquid-like phase of the gel remains highly dynamic. Unexpectedly, the translational motion is strongly enhanced, being the diffusion constants measured in the HEG between 40% and 90% higher than in the pure HES at the same temperature. The joint analysis of diffusion data and gelation-induced chemical shift variations is compatible with a scenario where the sample-spanning DBS network perturbs the local inter-HES interactions, and such interference is inversely proportional to either the strength of the pre-existing interactions or the number of C atoms of the alkyl chains. This enhanced mobility opens up new horizons toward applications requiring mobile systems, from synthesis and catalysis to drug delivery. In perspective, the thermoreversible gel-sol transition can also be exploited for 3D orienting applications. The insights gained here trigger more fundamental studies and pave the road for further improvements and development to the systems.

References

[1] D.J.G.P. Van Osch, C.H.J.T. Dietz, S.E.E. Warrag, M.C. Kroon, The curious case of hydrophobic deep eutectic solvents: a story on the discovery, design, and applications, ACS Sustain. Chem. Eng. 8 (2020) 10591–10612, https://doi.org/10.1021/acssuschemeng.0c00559.

[2] C. Florindo, L.C. Branco, I.M. Marrucho, Quest for green-solvent design: from hydrophilic to hydrophobic (deep) eutectic solvents, ChemSusChem 12 (2019) 1549–1559, https://doi.org/10.1002/cssc.201900147.

[3] D.O. Abranches, M.A.R. Martins, L.P. Silva, N. Schaeffer, S.P. Pinho, J.A.P. Coutinho, Phenolic hydrogen bond donors in the formation of non-ionic deep eutectic solvents: the quest for type v des, Chem. Commun. 55 (2019) 10253–10256, https://doi.org/10.1039/c9cc04846d.

[4] D.O. Abranches, J.A.P. Coutinho, Type V deep eutectic solvents: design and applications, Curr. Opin. Green Sustain. Chem. 35 (2022), 100612, https://doi.org/10.1016/j.cogsc.2022.100612.

[5] M.H. Zainal-Abidin, M. Hayyan, W.F. Wong, Hydrophobic deep eutectic solvents: current progress and future directions, J. Ind. Eng. Chem. 97 (2021) 142–162, https://doi.org/10.1016/j.jiec.2021.03.011.

[6] N. Schaeffer, M.A.R. Martins, C.M.S.S. Neves, S.P. Pinho, J.A.P. Coutinho, Sustainable hydrophobic terpene-based eutectic solvents for the extraction and separation of metals, Chem. Commun. 54 (2018) 8104–8107, https://doi.org/10.1039/c8cc04152k.

[7] N. Schaeffer, D.O. Abranches, L.P. Silva, M.A.R. Martins, P.J. Carvalho, O. Russina, A. Triolo, L. Paccou, Y. Guinet, A. Hedoux, J.A.P. Coutinho, Non-ideality in thymol + menthol type v deep eutectic solvents, ACS Sustain. Chem. Eng. 9 (2021) 2203–2211, https://doi.org/10.1021/acssuschemeng.0c07874.

[8] D.J.G.P. Van Osch, C.H.J.T. Dietz, J. Van Spronsen, M.C. Kroon, F. Gallucci, M. Van Sint Annaland, R. Tuinier, A search for natural hydrophobic deep eutectic solvents based on natural components, ACS Sustain. Chem. Eng. 7 (2019) 2933–2942, https://doi.org/10.1021/acssuschemeng.8b03520.

[9] J. Cao, E. Su, Hydrophobic deep eutectic solvents : the new generation of green solvents for diversified and colorful applications in green chemistry, J. Clean. Prod. 314 (2021), 127965, https://doi.org/10.1016/j.jclepro.2021.127965.

[10] R. Saini, S. Kumar, A. Sharma, V. Kumar, R. Sharma, S. Janghu, P. Suthar, Deep eutectic solvents: the new generation sustainable and safe extraction systems for bioactive compounds in agri food sector: an update, J. Food Process. Preserv. (2021) 1–39, https://doi.org/10.1111/jfpp.16250.

[11] P. Makoś, E. Słupek, J. Gębicki, Hydrophobic deep eutectic solvents in microextraction techniques–A review, Microchem. J. 152 (2020), 104384, https://doi.org/10.1016/j.microc.2019.104384.

[12] S. Wang, H. Cheng, B. Yao, H. He, L. Zhang, S. Yue, Z. Wang, J. Ouyang, Self-adhesive, stretchable, biocompatible, and conductive nonvolatile eutectogels as wearable conformal strain and pressure sensors and biopotential electrodes for precise health monitoring, ACS Appl. Mater. Interfaces 13 (2021) 20735–20745, https://doi.org/10.1021/acsami.1c04671.

[13] A.R. Hirst, B. Escuder, J.F. Miravet, D.K. Smith, High-tech applications of self-assembling supramolecular nanostructured gel-phase materials: from regenerative medicine to electronic devices, Angew. Chem. Int. Ed. 47 (2008) 8002–8018, https://doi.org/10.1002/anie.200800022.

[14] J. Le Bideau, L. Viau, A. Vioux, Ionogels, Ionic liquid based hybrid materials, Chem. Soc. Rev. 40 (2011) 907–925, https://doi.org/10.1039/c0cs00059k.

[15] L.C. Tomé, L. Porcarelli, J.E. Bara, M. Forsyth, D. Mecerreyes, Emerging iongel materials towards applications in energy and bioelectronics, Mater. Horiz. 8 (2021) 3239–3265, https://doi.org/10.1039/d1mh01263k.

[16] Y.R. Gao, J.F. Cao, Y. Shu, J.H. Wang, Research progress of ionic liquids-based gels in energy storage, sensors and antibacterial, Green Chem. Eng. 2 (2021) 368–383, https://doi.org/10.1016/j.gce.2021.07.012.

[17] J. Wang, S. Zhang, Z. Ma, L. Yan, Deep eutectic solvents eutectogels: progress and challenges, Green Chem. Eng. 2 (2021) 359–367, https://doi.org/10.1016/j.gce.2021.06.001.

[18] L.C. Tomé, D. Mecerreyes, Emerging ionic soft materials based on deep eutectic solvents, J. Phys. Chem. B 124 (2020) 8465–8478, https://doi.org/10.1021/acs.jpcb.0c04769.

[19] A.M. Navarro-Suárez, P. Johansson, Perspective—semi-solid electrolytes based on deep eutectic solvents: opportunities and future directions, J. Electrochem. Soc. 167 (2020), 070511, https://doi.org/10.1149/1945-7111/ab68d3.

[20] Y. Nahar, S.C. Thickett, Greener, faster, stronger: the benefits of deep eutectic solvents in polymer and materials science, Polymers 13 (2021) 1–24, https://doi.org/10.3390/polym13030447.

[21] J.D. Mota-Morales, R.J. Sánchez-Leija, A. Carranza, J.A. Pojman, F. del Monte, G. Luna-Bárcenas, Free-radical polymerizations of and in deep eutectic solvents: green synthesis of functional materials, Prog. Polym. Sci. 78 (2018) 139–153, https://doi.org/10.1016/j.progpolymsci.2017.09.005.

[22] L. Ren'Ai, K. Zhang, G. Chen, B. Su, J. Tian, M. He, F. Lu, Green polymerizable deep eutectic solvent (PDES) type conductive paper for origami 3D circuits, Chem. Commun. 54 (2018) 2304–2307, https://doi.org/10.1039/c7cc09209a.

[23] J.D. Mota-Morales, M.C. Gutiérrez, I.C. Sanchez, G. Luna-Bárcenas, F. Del Monte, Frontal polymerizations carried out in deep-eutectic mixtures providing both the monomers and the polymerization medium, Chem. Commun. 47 (2011) 5328–5330, https://doi.org/10.1039/c1cc10391a.

[24] C. Florindo, L.G. Celia-Silva, L.F.G. Martins, L.C. Branco, I.M. Marrucho, Supramolecular hydrogel based on a sodium deep eutectic solvent, Chem. Commun. 54 (2018) 7527–7530, https://doi.org/10.1039/c8cc03266a.

[25] J. Wu, T. Yin, Amphiphilic deep eutectic solvent based on lidocaine and lauric acid: formation of microemulsion and gel, Langmuir 38 (2022) 1170–1177, https://doi.org/10.1021/acs.langmuir.1c02837.

[26] K. Wang, H. Wang, J. Li, Y. Liang, X.Q. Xie, J. Liu, C. Gu, Y. Zhang, G. Zhang, C. Sen Liu, Super-stretchable and extreme temperature-tolerant supramolecular-polymer double-network eutectogels with ultrafast: in situ adhesion and flexible electrochromic behaviour, Mater. Horiz. 8 (2021) 2520–2532, https://doi.org/10.1039/d1mh00725d.

[27] S. Marullo, A. Meli, F. Giannici, F. D'Anna, Supramolecular eutecto gels: fully natural soft materials, ACS Sustain. Chem. Eng. 6 (2018) 12598–12602, https://doi.org/10.1021/acssuschemeng.8b04278.

[28] B. Saavedra, A. Meli, C. Rizzo, D.J. Ramón, F. D'Anna, Natural eutectogels: sustainable catalytic systems for C-C bond formation reactions, Green Chem. 23 (2021) 6555–6565, https://doi.org/10.1039/d1gc01647d.

[29] Y. Zhang, H. Wang, Q. Li, X. Chen, Gelation behavior and supramolecular chirality of a BTA derivative in a deep eutectic solvent, Soft Matter 18 (2022) 3241–3248, https://doi.org/10.1039/d2sm00028h.

[30] B. Zhang, H. Sun, Y. Huang, B. Zhang, F. Wang, J. Song, Multifunctional supramolecular eutectogels for self-healable conductive materials and interface lubrication, Chem. Eng. J. 425 (2021), 131518, https://doi.org/10.1016/j.cej.2021.131518.

[31] Y. Liang, K. Wang, J. Li, Y. Zhang, J. Liu, K. Zhang, Y. Cui, M. Wang, C. Sen Liu, Low-molecular-weight supramolecular adhesives based on non-covalent self-assembly of a small molecular gelator, Mater. Horiz. 9 (2022) 1700–1707, https://doi.org/10.1039/d2mh00156j.

[32] C. Gu, Y. Peng, J. Li, H. Wang, X.Q. Xie, X. Cao, C. Sen Liu, Supramolecular G4 eutectogels of guanosine with solvent-induced chiral inversion and excellent electrochromic activity, Angew. Chem. Int. Ed. 59 (2020) 18768–18773, https://doi.org/10.1002/anie.202009332.

[33] S. Marullo, A. Meli, N.T. Dintcheva, G. Infurna, C. Rizzo, F. D'anna, Environmentally friendly eutectogels comprising l-amino acids and deep eutectic solvents: efficient materials for wastewater treatment, Chempluschem 85 (2020) 301–311, https://doi.org/10.1002/cplu.202000017.

[34] F. Delbecq, P. Delfosse, G. Laboureix, C. Paré, T. Kawai, Study of a gelated Deep Eutectic solvent metal salt solution as template for the production of size-controlled small noble metal nanoparticles, Colloids Surf., A 567 (2019) 55–62, https://doi.org/10.1016/j.colsurfa.2019.01.035.

[35] L. Matthews, S. Ruscigno, S.E. Rogers, P. Bartlett, A.J. Johnson, R. Sochon, W.H. Briscoe, Fracto-eutectogels: SDS fractal dendritesviacounterion condensation in a deep eutectic solvent, Phys. Chem. Chem. Phys. 23 (2021) 11672–11683, https://doi.org/10.1039/d1cp01370j.

[36] Q. Cheng, A. Hao, P. Xing, Eutectogels as matrices to manipulate supramolecular chirality and circularly polarized luminescence, ACS Nano 16 (2022) 6825–6834, https://doi.org/10.1021/acsnano.2c01731.

[37] Y. Lan, M.G. Corradini, X. Liu, T.E. May, F. Borondics, R.G. Weiss, M.A. Rogers, Comparing and correlating solubility parameters governing the self-assembly of molecular gels using 1,3:2,4-dibenzylidene sorbitol as the gelator, Langmuir 30 (2014) 14128–14142, https://doi.org/10.1021/la5008389.

[38] B.O. Okesola, V.M.P. Vieira, D.J. Cornwell, N.K. Whitelaw, D.K. Smith, 1,3:2,4-Dibenzylidene-d-sorbitol (DBS) and its derivatives-efficient, versatile and industrially-relevant low-molecular-weight gelators with over 100 years of history and a bright future, Soft Matter 11 (2015) 4768–4787, https://doi.org/10.1039/c5sm00845j.

[39] J. Ruiz-Olles, P. Slavik, N.K. Whitelaw, D.K. Smith, Self-assembled gels formed in deep eutectic solvents: supramolecular eutectogels with high ionic conductivity, Angew. Chem. Int. Ed. 58 (2019) 4173–4178, https://doi.org/10.1002/anie.201810600.

[40] K.J. Winstanley, A.M. Sayer, D.K. Smith, Anion binding by catechols - an NMR, optical and electrochemical study, Org. Biomol. Chem. 4 (2006) 1760–1767, https://doi.org/10.1039/b516433h.

[41] K. Fan, L. Wang, W. Wei, F. Wen, Y. Xu, X. Zhang, X. Guan, Multifunctional self-healing eutectogels induced by supramolecular assembly for smart conductive materials, interface lubrication and dye adsorption, Chem. Eng. J. 441 (2022), 136026, https://doi.org/10.1016/j.cej.2022.136026.

[42] M.A.R. Martins, E.A. Crespo, P.V.A. Pontes, L.P. Silva, M. Bülow, G.J. Maximo, E.A.C. Batista, C. Held, S.P. Pinho, J.A.P. Coutinho, Tunable hydrophobic eutectic solvents based on terpenes and monocarboxylic acids, ACS Sustain. Chem. Eng. 6 (2018) 8836–8846, https://doi.org/10.1021/acssuschemeng.8b01203.

[43] C. Florindo, L. Romero, I. Rintoul, L.C. Branco, I.M. Marrucho, From phase change materials to green solvents: hydrophobic low viscous fatty acid-based deep eutectic solvents, ACS Sustain. Chem. Eng. 6 (2018) 3888–3895, https://doi.org/10.1021/acssuschemeng.7b04235.

[44] C.N. Prieto Kullmer, D. Ta, C.Y. Chen, C.J. Cieker, O. Annunziata, S.V. Dzyuba, Hexadecyl-containing organic salts as novel organogelators for ionic, eutectic, and molecular liquids, ACS Omega 4 (2019) 9400–9406, https://doi.org/10.1021/acsomega.9b00038.

[45] M.A.R. Martins, L.P. Silva, N. Schaeffer, D.O. Abranches, G.J. Maximo, S.P. Pinho, J.A.P. Coutinho, Greener terpene-terpene eutectic mixtures as hydrophobic solvents, ACS Sustain. Chem. Eng. 7 (2019) 17414–17423, https://doi.org/10.1021/acssuschemeng.9b04614.

[46] B. Joos, J. Volders, R.R. Da Cruz, E. Baeten, M. Safari, M.K. Van Bael, A.T. Hardy, Polymeric backbone eutectogels as a new generation of hybrid solid-state electrolytes, Chem. Mater. 32 (2020) 3783–3793, https://doi.org/10.1021/acs.chemmater.9b05090.

[47] M.L. Picchio, A. Gallastegui, N. Casado, N. Lopez-larrea, B. Marchiori, I. Agua, M. Criado-gonzalez, D. Mantione, R.J. Minari, D. Mecerreyes, Mixed ionic and electronic conducting eutectogels for 3D-printable wearable sensors and bioelectrodes, Adv. Mater. Technol. (2022), 2101680, https://doi.org/10.1002/admt.202101680.

[48] W.C. Lai, P.H. Huang, Self-assembly behaviors of dibenzylidene sorbitol hybrid organogels with inorganic silica, Soft Matter 13 (2017) 3107–3115, https://doi.org/10.1039/c6sm02853e.

[49] S. Grzesiek, E.D. Becker, Hydrogen Bonding, Encycl. Magn. Reson, 2007, https://doi.org/10.1002/9780470034590.emrstm0216.pub2.

[50] E. Posada, M.J. Roldán-Ruiz, R.J. Jiménez Riobóo, M.C. Gutiérrez, M.L. Ferrer, F. Del Monte, Nanophase separation in aqueous dilutions of a ternary DES as revealed by Brillouin and NMR spectroscopy, J. Mol. Liq. 276 (2019) 196–203, https://doi.org/10.1016/j.molliq.2018.11.139.

[51] M.E. Di Pietro, M. Tortora, C. Bottari, G. Colombo Dugoni, R.V. Pivato, B. Rossi, M. Paolantoni, A. Mele, Competition for water: hydrated choline chloride:urea vs choline acetate:urea deep eutectic solvents, ACS Sustain. Chem. Eng. 9 (2021) 12262–12273, https://doi.org/10.1021/acssuschemeng.1c03811.

[52] C.J. Smith II, D.V. Wagle, N. Bhawawet, S. Gehrke, O. Hollóczki, S.V. Pingali, H. O'Neill, G.A. Baker, Combined small-angle neutron scattering, diffusion NMR, and molecular dynamics study of a eutectogel: illuminating the dynamical behavior of glyceline confined in bacterial cellulose gels, J. Phys. Chem. B 124 (2020) 7647–7658, https://doi.org/10.1021/acs.jpcb.0c04916.

[53] C. Zeng, H. Zhao, Z. Wan, Q. Xiao, H. Xia, S. Guo, Highly biodegradable, thermostable eutectogels prepared by gelation of natural deep eutectic solvents using xanthan gum: preparation and characterization, RSC Adv. 10 (2020) 28376–28382, https://doi.org/10.1039/d0ra03390a.

[54] K. Van Aken, L. Strekowski, L. Patiny, EcoScale, a semi-quantitative tool to select an organic preparation based on economical and ecological parameters, Beilstein J. Org. Chem. 2 (2006) 1–7, https://doi.org/10.1186/1860-5397-2-3.

[55] F. D'Amico, C. Papucci, D. Franchi, G. Reginato, M. Calamante, L. Zani, A. Dessì, A. Mordini, Sustainable Pd-catalyzed direct arylation of thienyl derivatives with (Hetero)aromatic bromides under air in deep eutectic solvents, ACS Sustain. Chem. Eng. 10 (2022) 3037–3047, https://doi.org/10.1021/acssuschemeng.1c08466.